URSI - RCRS 2022, IIT (Indore), India, 1 - 4 December, 2022

Artificial Magnetic Conductor backed Printed Monopole MIMO Antenna for Millimeter-Wave 5G WBAN Applications

Priyank Mishra*, Praneet Jain, Maharana Pratap Singh, and Saptarshi Ghosh
Department of Electrical Engineering, Indian Institute of Technology Indore, M.P. – 453552, India.

Abstract

A low profile, high gain, and with improved safety features artificial magnetic conductor (AMC) backed printed monopole multiple-input-multiple-output (MIMO) antenna for millimeter-wave (mm-wave) 5G wireless body area network (WBAN) applications is presented. The proposed design consists of a printed monopole in the top layer with a partial ground plane. A single antenna element along with the connector model has initially been designed with a detailed analysis and subsequently, a two-port MIMO antenna backed by an AMC structure is realized. The AMC structure consists of 5 × 4 unit cells that are made up of two interconnected I-shaped slots etched out of a metallic patch (Jerusalem Cross). With the use of AMC, the antenna gain at 28 GHz increases by 4.89 dBi due to the suppression of surface wave. The specific absorption rate (SAR) and power density are also reduced by the AMC. The performance of the AMC-backed antenna remains consistent in the two-port MIMO antenna having an overall dimension of 25 × 40 × 3.7 mm3. In addition, several MIMO parameters are calculated, and their results are found to be suitable for 5G WBAN applications. Finally, the antenna prototype as well as the AMC are fabricated and their measured results conform to the simulated responses, validating the proposed concepts.

1. Introduction

Widespread enrollment of 5th generation (5G) wireless technology is on the way. The objective is to fulfill the need of higher data rates, low latency, and high user density. To attain these objectives, the mm-wave spectrum, particularly the 24-28 GHz, 37-39 GHz, and 60 GHz bands have been suggested [1], [2]. Because of high absorption loss at 60 GHz, 28 GHz and 38 GHz bands are the most sought-after bands for mm-wave 5G communication [3]. However mm-wave spectrum poses its own challenges such as high path loss and significant atmospheric absorptions. Therefore, multiple-input-multiple-output (MIMO) technology is being implemented in the mm-wave range, as it not only promises higher data rates but benefits of diversity as well.

Microstrip patch antennas are of obvious choices for wearable applications as they are low profile, lightweight, conformable in nature, and easy to implement. However, patch antennas suffer from low impedance bandwidth and partial ground structure or defective ground structure (DGS) has been commonly used to enhance the bandwidth. But, this partial ground plane makes the antennas have radiation on the back side as well. This results in lower radiation efficiency and poor operating gain. Further, the backward radiation is harmful to human tissues, as it penetrates through them. To resolve this problem, the artificial magnetic conductor (AMC) is a promising choice as it not only reduces the backside radiation, but also improves the operating gain. In addition, the AMC can be placed in close proximity to the antenna geometry unlike a perfect electric conductor (PEC), which needs to be placed at least at a distance of 0.25λo from the antenna [4].

Recently, a variety of AMC surfaces are used to enhance the performances of microstrip patch antennas. In Ref. [5], an annular slot antenna with an AMC reflector is presented. Three different AMC structures and their usage as a reflector are demonstrated as well as compared with a PEC reflector with the help of an antenna prototype. However, the said AMC structures are meant for narrow-band applications only. In Ref. [6], a printed dipole antenna backed with a rhomboid AMC is suggested for vehicular wireless communication. The geometry is studied with and without the presence of an AMC structure and a performance enhancement is observed in terms of a size decrement of 42.3%, gain improvement by 8.4 dB, and resulting in a unidirectional radiation pattern. The use of AMC has improved the gain by 1.9 dB in addition to the reduction of backside radiation by 8 dB as well as power density to 10 W/m^2 (from an initial value of 200 W/m^2) in Ref. [7]. However, the band of operation is comparatively narrow and centered around 24 GHz.

In this study, a detailed discussion of a printed monopole MIMO antenna backed by a broadband AMC design for 5G wearable network working at 28 GHz is reported. A careful design of the AMC structure has led to a significant improvement in the performance of the antenna geometry in terms of operating gain, impedance bandwidth, and radiation direction. The antenna design is further expanded to a two-port MIMO configuration for obtaining a high data rate and increased channel capacity. The antenna geometry is fabricated with and without AMC structures and their measured responses conform to those of the simulated results, thereby validating the proposed concepts.

2. DESIGN OF AMC BACKED PRINTED MONOPOLE MIMO ANTENNA

The schematic of the proposed single antenna design is illustrated in Fig. 1. It consists of a printed monopole element on the top side of the substrate, whereas the bottom side contains a partial ground plane. The radiator is fed by a 50 Ω microstrip line and Rogers RO 4003(TM) substrate has been used as the constituent dielectric, which has a relative permittivity of 3.55 and a loss tangent of 0.0027. The thickness of the substrate is taken as 0.3 mm. The overall dimensions of the proposed geometry are 15 mm x 15 mm. Other physical dimensions are mentioned in Fig. 1.

The proposed geometry is simulated in Ansys HFSS 2020 software. The simulated result exhibits a -10 dB impedance bandwidth of 4.4 GHz (25 -29.4 GHz) centering around 28 GHz. The structure is also fabricated using LPKF Protomat S104 equipment. The measured -10 dB impedance bandwidth is found to be 5.34 GHz (26.68-32.02 GHz). Both the simulated and measured results are compared in Fig. 2 and they achieve good conformity between them.

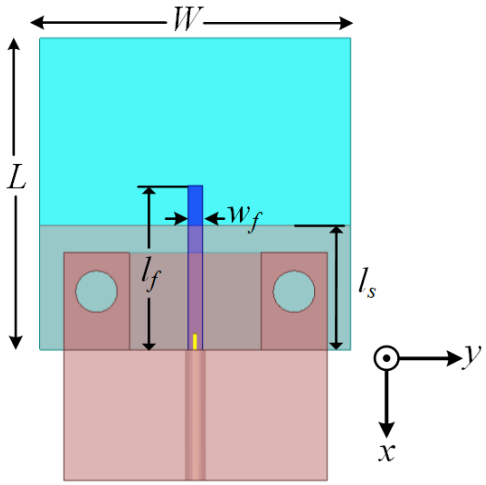

Figure 1. Diagrammatic representation of the proposed single monopole antenna. The optimized dimensions are: L = W= 15, l_f = 7.9, W_f = 0.7, l_S = 6 (units: mm).

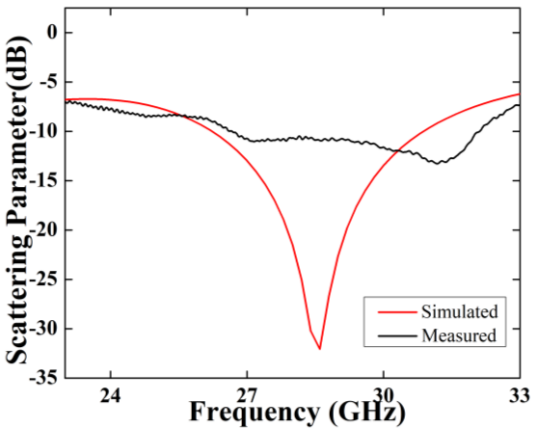

Figure 2. Simulated and measured reflection coefficient (S_{11}) response of the proposed single antenna.

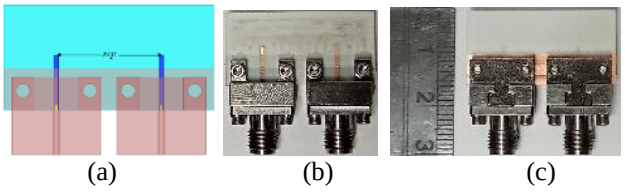

Figure 3. (a) Geometry of the proposed 1 × 2 MIMO antenna with *sep* = 15 mm. Photograph of the fabricated MIMO antenna: (b) top layer, and (c) bottom layer.

After presenting the single antenna design, the two-port MIMO antenna geometry is depicted in Fig. 3(a), where the elements are placed side by side. The geometric dimensions and the substrate properties remain the same, whereas the separation (sep) between the monopoles is considered as 15 mm, based on the optimized responses. The top and bottom layers of the fabricated MIMO antenna prototype are depicted in Figs. 3(b) and 3(c).

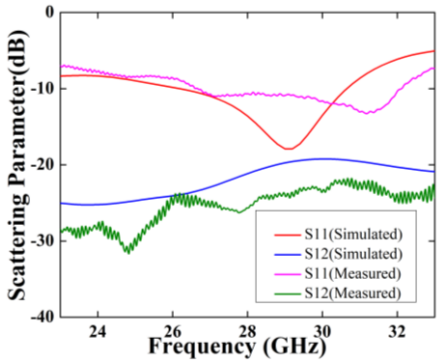

Figure 4. Simulated and measured S-parameter plots of the proposed 2-port MIMO antenna.

The simulated and measured S-parameters for 1x2 MIMO are shown in Fig. 4. It is observed from the measured results that the antenna is working at a frequency band from 26.68 GHz to 32.02 GHz with S_{11} lower than -10 dB. The isolation is also observed to be above 18 dB throughout the operating range. The simulated and the measured results achieve good conformity between them.

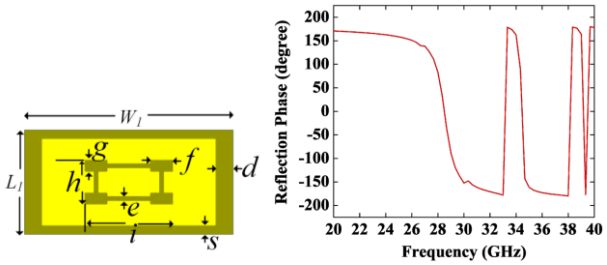

Figure 5. (a) The unit cell geometry of the proposed AMC, and (b) its simulated reflection phase characteristics. The dimensions are: L_1= 5, W_1=*10*, s=0.41, d=0.82, e = 0.2, f=1.04, g=0.52, h=2.08, i=4.17 (units: mm).

The proposed AMC is made of two metallic layers sandwiching a single layer dielectric of Rogers RO 4003(TM) substrate of thickness 0.3 mm (relative

permittivity of 3.55 and loss tangent of 0.0027). The top layer is two interconnected I-shaped slots etched out of a metallic patch (Jerusalem Cross), whereas the bottom layer is complete metal laminated. The unit cell geometry is presented in Figs. 5(a) and its corresponding reflection phase is displayed in Fig. 5(b). It can be observed that the reflection phase cross the 0º level at around 28 GHz. While considering the phase range from -90º to +90º, a wide bandwidth is thus obtained around 28 GHz which will be used in improving the antenna performance.

The designed printed monopole MIMO antenna is placed above the AMC array as shown in Fig 6(a) with 3.4 mm separation between them. The separation is selected such that connector of antenna can be accommodated in the space between antenna and AMC. The array size (5×4) is chosen in such a way so as to completely cover the 1x2 MIMO antenna. The antenna along with AMC is shown in Fig 6(b). The simulated and measured S-parameter results are presented in Fig 7. It is observed that the MIMO antenna with AMC exhibits a -10 dB impedance bandwidth of 2.10 GHz (27.10–29 GHz). The measured result demonstrates that there is good conformity between measured and simulated results.

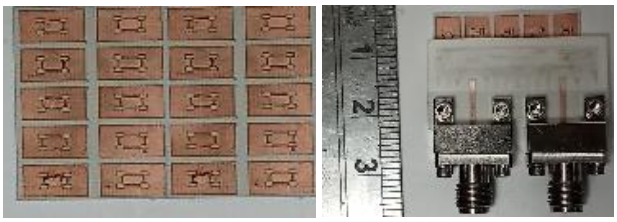

(a) (b)

Figure 6. Photographf of the (a) fabricated AMC array (5 × 4), and (c) complete MIMO antenna with AMC.

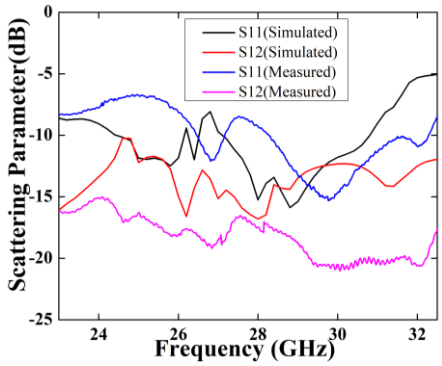

Figure 7. Simulated and measured S_{11} and S_{12} response of the proposed MIMO antenna with AMC.

3. RESULTS AND DISCUSSION

The simulated 3D far-field gain pattern for the proposed antenna is shown in Fig. 8(a) for 28 GHz. It can be witnessed that the peak gain of 4.36 dBi is obtained at 28 GHz. It is also evident that the antenna is radiating in the broadside direction. With the introduction of the AMC, the radiation pattern of the antenna becomes unidirectional as it acts as a reflector to main radiator. The simulated 3D far-field gain patterns for the proposed antenna with AMC is shown in Fig. 8(b) for 28 GHz. It can be witnessed that the peak gain of 9.25 dBi is obtained at 28 GHz frequency. It is further witnessed from Fig 9(a) that the total gain at 27 GHz or 29 GHz is reduced as compared to 28 GHz. This is possibly due to the fact that AMC has limited bandwidth. So it cannot maintain uniform phase for all frequencies away from its center frequency and so the radiation pattern becomes frequency dependent [8].

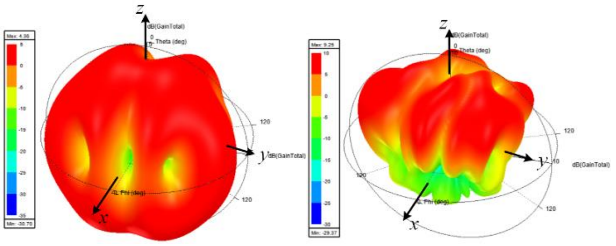

(a) (b)

Figure 8. Simulated 3D far field gain pattern of the antenna: (a) without AMC, and (b) with AMC at 28 GHz.

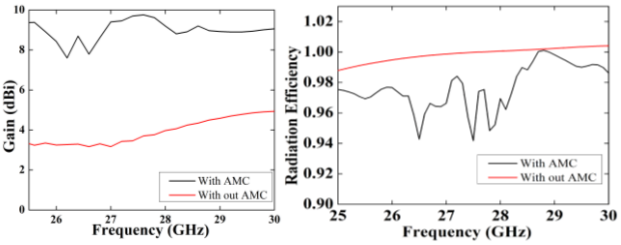

(a) (b)

Figure 9. (a) Simulated gain (without and with AMC), and (b) simulated radiation efficiency (without and with AMC).

Important parameters like envelope correlation constant (ECC), total active reflection constant (TARC) and channel capacity loss (CCL) for confirming the MIMO antenna (with AMC) performance have been examined. The parameters are determined from scattering coefficients, using equations mentioned in [9]. The ECC, which is a measure of correlation or isolation between the radiation patterns of the proposed MIMO antenna, has been achieved well below the desired limit at both the operating frequencies (around 28 GHz and 38 GHz), as shown in Fig. 10(a). The TARC, which is the ratio of total reflected power to the total incident power, is obtained within the desired value, as depicted in Fig. 10(b). The CCL which measures the rate of information that can be reliably transmitted over the communication channel is obtained within the desired value of less than 0.5 bits/seconds/Hertz in the proposed MIMO antenna. The response is depicted in Fig. 10(c). All the parameters are determined from simulated as well as measured from S-parameters, and they have close conformity around the operating frequency.

The proposed design is compared with earlier reported AMC based antenna structures. Different antenna parameters are tabulated in Table I and it is observed that

the designed MIMO antenna shows significantly higher gain with a lower form factor and good safety performance, with respect to earlier reported MIMO antenna structures.

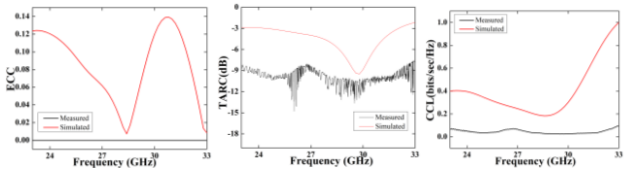

Figure 10. Simulated and measured MIMO performance parameters of the proposed 1 × 2 MIMO antenna: (a) ECC, (b) TARC, and (c) CCL.

Refs.	Size (mm × mm × mm) Dimension (λ_o)	Freq band (GHz)	Gain (dBi)	1-g average SAR (W/Kg)	SPD (W/m^2)
[7]	19.04x15.06x_ (1x2 MIMO)	24	6	-	2428.3
[20]	30 x50 x3	4.8–6.7	7.6	0.22	-
[26]	46 x 46 x 2.4	2.4	7.8	0.0368	-
[27]	102 x 68 x 3.6	4.30–5.90	6.12	0.37	-
[28]	72x72x11	4.90–5.5	6.2	-	-
Proposed Antenna	25 x 40 x 3.7 (1X2 MIMO)	28	9.25	0.112 (three layer)	2.38 (three layer)

4. CONCLUSION

In this work, a printed monopole MIMO antenna backed with Artificial Magnetic Conductor (AMC) has been presented for mm-wave 5G (28GHz) WBAN applications. The introduction of the AMC on backside of antenna enhances the peak gain by 4.89 dBi. Moreover, the backside electromagnetic radiation of antenna on the human body is examined with SAR and SPD using a realistic human body model. The value of SAR and SPD of suggested antenna (with AMC) is found to be drastically reduced with the use of AMC. The geometries are fabricated and the measured responses are in reasonable conformity with those of the simulated results. The proposed MIMO antenna is suitable for wearable body area network applications at the mm-Wave frequencies.

6. Acknowledgements

This work was supported in part by Science and Engineering Research Board, India, under Project TTR/2021/000106 and Department of Science & Technology, under Project DST/INT/JSPS/P-329/2021.

7. References

1. W. Hong, K.-H. Baek, and S. Ko, “Millimeter-wave 5G antennas for smartphones: Overview and experimental demonstration,” IEEE Trans. Antennas Propag., vol. 65, no. 12, pp. 6250–6261, Dec. 2017.

2. S. Islam, M. Zada and H. Yoo, "Low-Pass Filter Based Integrated 5G Smartphone Antenna for Sub-6-GHz and mm-Wave Bands," in *IEEE Transactions on Antennas and Propagation*, vol. 69, no. 9, pp. 5424-5436, Sept. 2021.

3. A. Khabba, S. Ibnyaich, and M. M. Hassani, “A new design of multi-band antenna array for 5G cellular phones applications” Proceedings of *2nd International Conference of Computer Science and Renewable Energies (ICCSRE), IEEE*, Agadir, Morocco, 2019.

4. W. T. Hsieh, T. H. Chang, and J. F. Kiang, “Dual-band circularly polarized cavity-backed annular slot antenna for GPS receiver,” *IEEE Trans. Antennas Propag.*, vol. 60, pp. 2076-2080, 2012.

5. S. Dutta and K. Agarwal, “Unidirectional AMC reflector backed L-band annular slot antenna,” *2015 IEEE International Conference on Microwaves, Communications, Antennas and Electronic Systems (COMCAS)*, 2015, pp. 1-5.

6. H. Malekpoor and M. Hamidkhani, “Performance enhancement of low-profile wideband multi-element MIMO arrays backed by AMC surface for vehicular wireless communications,” *IEEE Access*, vol. 9, pp. 166206-166222, 2021.

7. A. Iqbal *et al*., “Electromagnetic bandgap backed millimeter-wave MIMO antenna for wearable applications,” *IEEE Access*, vol. 7, pp. 111135-111144, 2019.

8. A. Ahlbom, “Guidelines for limiting exposure to time-varying electric, magnetic, and electromagnetic fields (up to 300 GHz),” *Health Phys.*, vol. 74, no. 4, pp. 494–522, Apr. 1998.

9. M. S. Sharawi, “Printed multi-band MIMO antenna systems and their performance metrics,” *IEEE Antennas Propag. Mag.*, vol. 55, no. 5, pp. 218–232, Oct. 2013.

20. A. Verma, R. K. Arya, R. Bhattacharya, and S. N. Raghava, “Compact PIFA antenna with high gain and low SAR using AMC for WLAN/C-band/5G applications,” *IETE Journal of Research*, 2021.

26. A. Y. I. Ashyap *et al*., “Compact and low-profile textile EBG-based antenna for wearable medical applications,” *IEEE Antennas Wireless Propag. Lett.*, vol. 16, pp. 2550-2553, 2017.

27. A. Alemaryeen, and S. Noghanian, “On-body low-profile textile antenna with artificial magnetic conductor,” *IEEE Trans. Antennas Propag.*, vol. 67, pp. 3649–3656, 2019.

28. S. X. Ta, and I. Park, “Dual-band low-profile crossed asymmetric dipole antenna on dual-band AMC surface,” *IEEE Antennas Wirel. Propag. Lett.*, Vol. 13, pp. 587–590, 2014.